IEEE Photonics Journal
An IEEE Photonics Society Publication

High-Performance Red Lasers With Low Beam Divergence

Volume 1, Number 3, September 2009

Bocang Qiu
O. P. Kowalski
Stewart McDougall, Member, IEEE
B. Schmidt
John H. Marsh, Fellow, IEEE

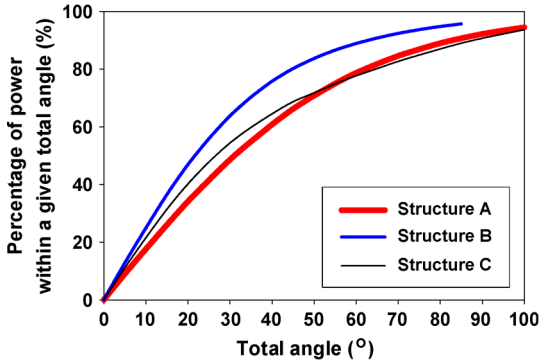

DOI: 10.1109/JPHOT.2009.2030159
1943-0655/$26.00 ©2009 IEEE

High-Performance Red Lasers With Low Beam Divergence

Bocang Qiu, O. P. Kowalski, Stewart McDougall, *Member, IEEE*, B. Schmidt, and John H. Marsh, *Fellow, IEEE*

Intense Ltd., G72 0BN Glasgow, U.K.

DOI: 10.1109/JPHOT.2009.2030159
1943-0655/$26.00 ©2009 IEEE

Manuscript received July 30, 2009. First published Online August 10, 2009. Current version published August 28, 2009. This work was carried out while John H. Marsh was on secondment from the University of Glasgow. Corresponding author: B. Qiu (e-mail: bocang_qiu@intenseco.com).

Abstract: We report the design and fabrication of high-performance 650-nm lasers using a novel wafer structure that offers substantially independent control of the vertical far field and of the optical confinement factor. By incorporating a graded V-shaped layer into the epitaxial structure, a low divergence can be realized while retaining high optical overlap with the quantum wells and, therefore, a low threshold current. Broad-area lasers (BALs) were fabricated for a range of designs, and close agreement was obtained between the modeling and the experiment.

Index Terms: Red lasers, InGaAlP, low beam divergence.

1. Introduction

Visible laser diodes emitting in the wavelength range 630–660 nm were first demonstrated in the mid 1980s [1], [2]. They are now used in a wide variety of applications including pumping solid-state lasers, laser projection and displays, data storage systems, photodynamic therapy and digital printing. It is highly desirable that a laser structure has a low threshold current, and this becomes an essential requirement in some applications, particularly at the short end of the wavelength range where the characteristic temperature T_0 is lowest. When using monolithic arrays in printing applications [3], for example, thermal crosstalk, which is defined as optical power change for a given emitter in a laser array when other adjacent lasers are switched on, is highly sensitive to the threshold current, and a low threshold current becomes an absolute necessity. On the other hand, it is often required that the laser has a low beam divergence, because this reduces the numerical aperture (NA) of the optical train, maximizing coupling efficiency and relaxing coupling tolerances. The laser threshold current is strongly dependent on the optical confinement factor Γ, defined as the overlap integral of an optical mode with the quantum wells (QWs), and a large value of Γ leads to a lower threshold current. Low beam divergence is normally achieved by increasing the spot size of the optical mode [4], leading to a decrease in Γ, so there is generally a compromise between threshold current and vertical beam divergence. In red laser materials, the situation is made worse by the fact that the material gain is reduced at short wavelengths. As a result, the threshold current of red lasers is much more sensitive to Γ than their longer wavelength (e.g., 980 nm) counterparts. In order to minimize the threshold current, one has to maximize the modal gain by maximizing the optical confinement factor; this inevitably leads to an increase in the beam divergence in the vertical direction, or in other words, the vertical far field (VFF).

In this paper, we propose a novel approach [5], [6] which can significantly reduce the beam divergence while having little impact on the laser threshold current. A conventional red laser

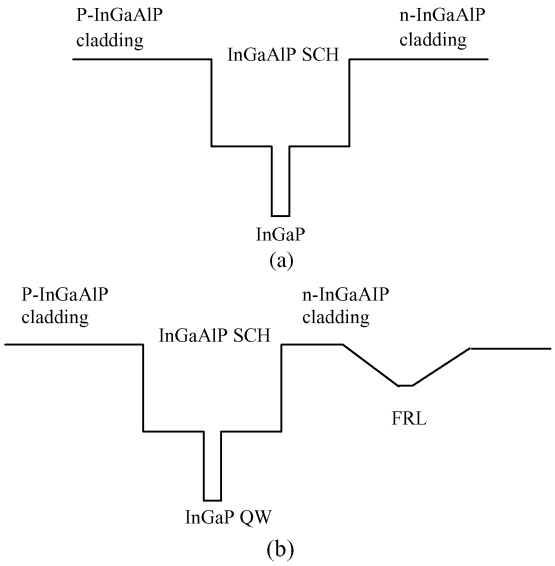

Fig. 1. (a) Conventional structure. (b) Proposed structure with FRL.

structure is illustrated in Fig. 1(a). As can be seen, the wafer structure consists of an InGaP QW with tensile or compressive strain, separate confinement heterostructure (SCH) waveguide layers, and lower (n-side) and upper (p-side) cladding layers. In order to realize a low threshold current in such conventional structures, the VFF is typically around 40°, measured at full width of half maximum (FWHM). The proposed new wafer structure [see Fig. 1(b)] is identical to the conventional case, except that an extra layer for reducing the VFF is inserted in the lower cladding layer; this layer is hereafter refer to as a far-field reduction layer (FRL). The proposed structure allows us to independently control both threshold current and beam divergence. It has been previously demonstrated that a V-profile FRL offers improved growth tolerances compared to a step-like FRL [5], and we have therefore focused on structure optimization using a V-profile FRL. Modeling of the designed structure shows that the VFF can be reduced from $\sim$38° for a conventional structure to $\sim$22°, with the threshold current increasing by only about 3%. Wafer structures with and without the FRL were grown, along with a third structure which employed a conventional method for reducing the far-field divergence, namely by reducing the thickness of the SCH layers. Broad-area lasers (BALs) have been fabricated and assessed and good agreement is obtained between the modeling predictions and experimental results.

2. Modeling

As can be seen in Fig. 1(b), the FRL is incorporated in the n-cladding layer. The FRL is essentially a much weaker waveguide compared with the waveguide core surrounding the active QWs and serves to expand the optical near field slightly in the vertical direction and to suppress higher order lateral mode lasing [5]. Expansion of the near field leads to a reduction of the corresponding far field through Fourier transformation. A commercially available software package (FIMMWAVE) was used to model the near-field and far-field patterns. The refractive indices of the materials used in the model were found using the formula proposed by Afromowitz [7], and are plotted in Fig. 2. The FRL was then optimized to deliver the required beam divergence and optical confinement factor. The parameters used for the optimization were the thickness of the FRL, the separation between the SCH and FRL, and the material composition at the mid-point of the FRL. Fig. 3 shows the dependence of the VFF and Γ on the FRL thickness, with the separation between the FRL and SCH being fixed at 620 nm. It can be seen that with increasing FRL thickness, the far field decreases monotonically from 38° to a value as low as 24°, while the optical confinement factor Γ only experiences a marginal change. This is because the FRL primarily affects that part of the near-field

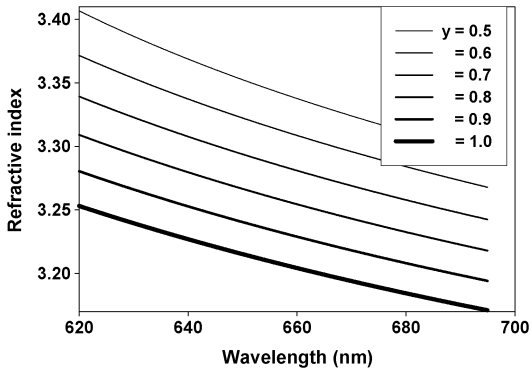

Fig. 2. Refractive indexes for InGaAlP materials.

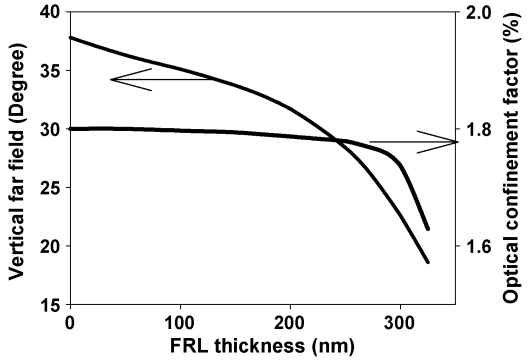

Fig. 3. Dependence of optical confinement and beam divergence on the FRL.

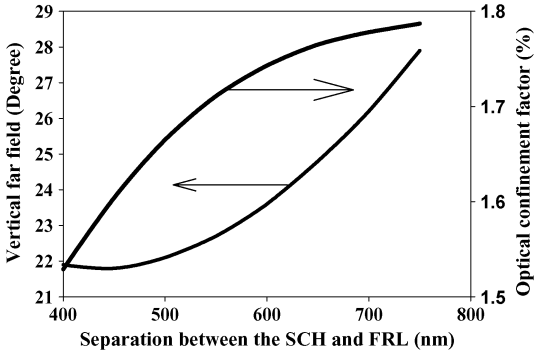

Fig. 4. Dependence of optical confinement and beam divergence on the separation between the FRL and SCH layer.

distribution which is far away from the QW region. A further increase in the FRL thickness results in a substantial decrease in optical confinement or even in a movement of the optical mode from the waveguide core to the FRL, and careful design has to be exercised to avoid such an occurrence. Fig. 4 shows the effect of separation between the SCH and FRL on the laser performance.

To evaluate the effect of the FRL on threshold current, the structures were simulated using a detailed laser model which was validated using measured data from red laser structures. The model starts with the calculation of material gain for a given structure, and the threshold current is then calculated using, as an input, the optical confinement factor Γ calculated using FIMMWAVE. The increase in threshold current for a 75-μm-wide, 1-mm-long metal stripe laser is plotted in Fig. 5 as a function of beam divergence (VFF) for an FRL and for a conventional design. It can be seen that the

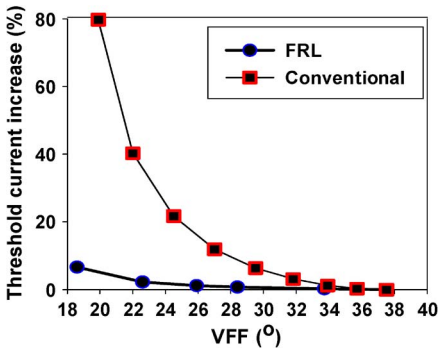

Fig. 5. Calculated threshold current as function of beam divergence.

TABLE 1
Brief summary of three different structures

Design	Predicted Γ (%)	Predicted VFF (°)
Structure A	1.80	37.2
Structure B	1.41	23.4
Structure C	1.75	24.0

FRL enables the beam divergence to be reduced by a factor > 2 with only a very limited increase in laser threshold current (< 5%). In contrast, the increase in threshold current is much more significant (> 80%) when using the conventional approach of reducing the thickness of SCH layers forming the waveguide core.

3. Fabrication and Test

To verify the theoretical modeling, three different structures were grown. The first (referred to as structure A) was a standard structure with a VFF of around 37°; the second a structure had a reduced VFF of about 24° using the conventional approach of reducing waveguide *thickness* (Structure B), and the third (Structure C) was identical to structure A except that an FRL was incorporated in the n-cladding layer. A brief summary of the structures is given in Table 1. Wafers were grown using metal organic vapor phase epitaxy (MOVPE) on an n^+ GaAs substrate mis-oriented by 10° toward ⟨111⟩. The QW was a compressively strained InGaP layer surrounded by $(Al_{0.6}Ga_{0.4})_{0.51}In_{0.49}P$ SCH layers. The cladding layers were $Al_{0.51}In_{0.49}P$, and the material composition at the bottom of the FRL was $(Al_{0.70}Ga_{0.30})_{0.51}In_{0.49}P$ with the total thickness being 600 nm. The wafer was completed by growing lower (n-side) and upper (p-side) *InAlP* cladding layers. Simple metal stripe lasers were fabricated to evaluate the material performance. The metal stripe was 75 μm wide, and lasers were cleaved to a number of cavity lengths. The as-cleaved lasers were tested under pulsed conditions at room temperature. Fig. 6 plots the VFF of the three structures at same the power level, and Fig. 9 shows the *L–I* characteristics. The emission wavelengths were very close, being 656 nm, 654 nm and 656 nm under pulsed conditions at 25 °C for structures A–C, respectively. The temperature sensitivity parameter of the threshold current, T_0, was deduced from measurements on BALs and had a value of about 63 K for all three structures. The slope efficiencies (per facet) were 0.53 W/A, 0.46 W/A, and 0.50 W/A for structures respectively.

It can be seen from Fig. 6 that the FWHM values of VFF are 37°, 24°, and 23.5° for structures A–C, respectively, which are very close to the designed values (see Table 1). By integrating the far-field profiles in Fig. 6, one can calculate the percentage of total power within a given total coupling angle (see Fig. 7). Obviously, at small NAs, Structure C offers better coupling compared with structure A; however the coupling for structure C becomes similar to or slightly poorer than that of

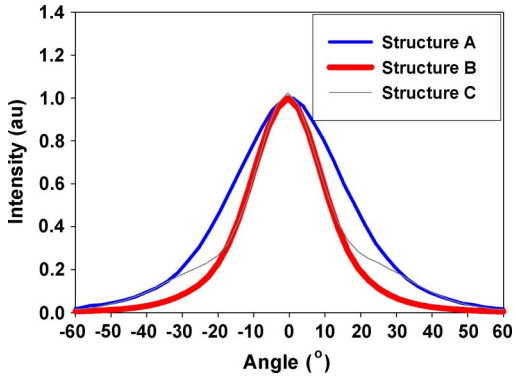

Fig. 6. Measured VFF for three different structures.

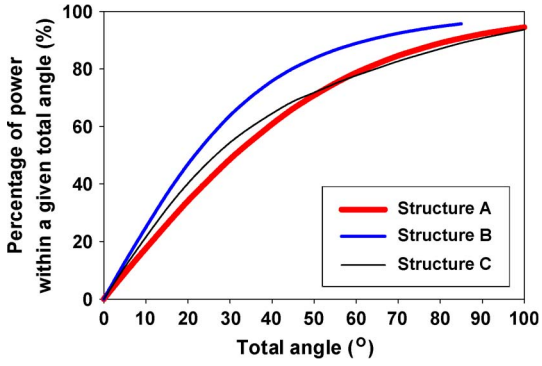

Fig. 7. Percentage of total power within a given total coupling angle.

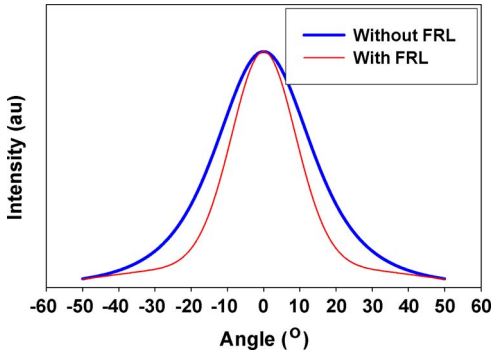

Fig. 8. Improved far-field profile by simulation.

structure A when the NA is large. The reason for the convergence in coupling at large NAs is that the far-field profile of structure C becomes the same as that of structure A at large divergence angles. The non-Gaussian far-field profile for structure C was predicted by the model, and is caused by very strong optical confinement in the waveguide core. By modifying the waveguide core, for example by employing a graded waveguide and reducing the waveguide confinement slightly, the profile should become more Gaussian and this is illustrated in Fig. 8, in which the VFF values for the structure with and without FRL are 22.5° and 31.4°, respectively. However, our initial design strategies were to achieve as large Γ as possible and, in the meantime, to demonstrate the possibility of reducing beam divergence by incorporating an FRL. From the *L–I* plots (see Fig. 9), we can see that structures A and B have the smallest and largest threshold current, respectively, while the threshold current for structure C lies in between that of A and B. The measured threshold current for structure C

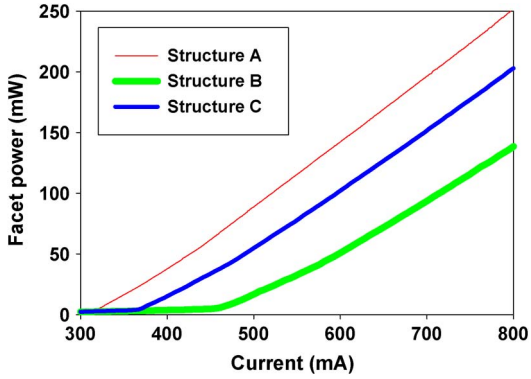

Fig. 9. Measured *L–I* plots for three different structures.

is 14% larger than that for structure A, which compares favorably with the 48% increase in measured threshold current for reference structure B. This follows the trend predicted by the modeling, although the increases in threshold current for both structures B and C are larger than predicted; the increase in calculated threshold is only about 2% for structure C and 30% for structure B. The discrepancies between modeling and measurement are most probably to variations associated with epitaxy in the InGaAlP system, where small errors in the material compositions of the waveguide core and cladding layers result in significant changes in Γ and, hence, in the threshold current.

4. Summary

We have demonstrated that the vertical beam divergence at FWHM of a red laser can be significantly reduced by incorporating an FRL into a laser structure with little impact on laser performance. Experimental results confirm our design concept. We have demonstrated that, by using an FRL, it is possible to reduce the VFF from 37° to 24° with only a 14% penalty in threshold current.

References

[1] M. Ikeda, Y. Mori, H. Sato, K. Kaneko, and N. Watanabe, "Room temperature continuous wave operation of an AlGaInP double heterostructure laser grown by atmospheric pressure metalorganic chemical vapor deposition," *Appl. Phys. Lett.*, vol. 47, no. 10, pp. 1027–1028, Nov. 1985.

[2] K. Kobayashi, S. Kawata, A. Gomyo, I. Hino, and T. Suzuki, "Room temperature CW operation of AlGaInP double heterostructure visible lasers," *Electron. Lett.*, vol. 21, no. 20, pp. 931–932, Sep. 1985.

[3] O. P. Kowalski, S. D. McDougall, B. C. Qiu, G. H. Masterton, M. L. Armstrong, S. Robertson, S. Caldecott, and J. H. Marsh, "Ultra-fine pitch individually addressable visible laser arrays for high speed digital printing applications," in *Proc. SPIE—Novel In-Plane Semiconductor Lasers VIII (Photonics West)*, 2009, vol. 7230, pp. 72301J-1–72301J-8.

[4] D. Botez, "Design considerations and analytical approximations for high continuous power, broad-waveguide diode lasers," *Appl. Phys. Lett.*, vol. 74, no. 21, pp. 3102–3104, 1999.

[5] B. Qiu, S. McDougall, G. Bacchin, X. Liu, and J. H. Marsh, "Design and fabrication of low beam divergence and high kink-free power lasers," *IEEE J. Quantum Electron.*, vol. 41, no. 9, pp. 1124–1130, Sep. 2005.

[6] J. M. Verdiell, M. Ziari, and D. F. Welch, "Low-loss coupling of 980 nm GaAs laser to cleaved singlemode fibre," *Electron. Lett.*, vol. 32, no. 19, pp. 1817–1818, Sep. 1996.

[7] M. A. Afromowitz, "Refractive index of $Ga_{1-x}Al_xAs$," *Solid State Commun.*, vol. 15, pp. 59–63, 1974.